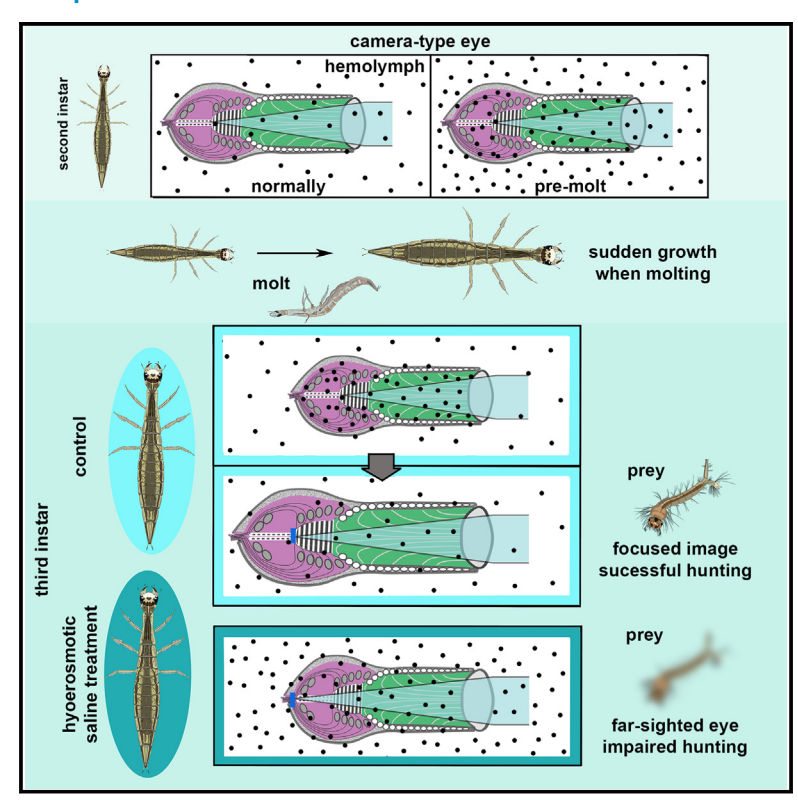
Current Biology

Osmosis as nature's method for establishing optical alignment

Graphical abstract



Authors

Shubham Rathore, Amartya T. Mitra, Ruby Hyland-Brown, Augusta Jester, John E. Layne, Joshua B. Benoit, Elke K. Buschbeck

Correspondence

shubham.rathore@nih.gov (S.R.), elke.buschbeck@uc.edu (E.K.B.)

In brief

Rathore et al. find that the post-molt rapid growth of camera-type eyes of *Thermonectus marmoratus* larvae is driven by osmotic processes. Supporting evidence suggests that endogenous hemolymph osmotic changes correlate with support cell swelling. Manipulating the osmotic environment leads to farsighted larvae with behavioral deficits.

Highlights

- Post-molt eye growth in insect larvae involves rapid support cell swelling
- Support cell expansion coincides with endogenous hemolymph osmotic changes
- Interfering with osmotic processes results in farsightedness and behavioral deficits
- Osmoregulation may be of ubiquitous importance for properly focused eyes



Current Biology



Report

Osmosis as nature's method for establishing optical alignment

Shubham Rathore, 1,2,3,* Amartya T. Mitra, 1 Ruby Hyland-Brown, 1 Augusta Jester, 1 John E. Layne, 1 Joshua B. Benoit, 1 and Elke K. Buschbeck 1,4,*

- ¹Department of Biological Sciences, University of Cincinnati, Cincinnati, OH 45221, USA
- ²Present address: Section on Light and Circadian Rhythms (SLCR), National Institute of Mental Health, NIH, Bethesda, MD 20892, USA
- ³X (formerly Twitter): @ShubhamTRathore
- ⁴Lead contact
- *Correspondence: shubham.rathore@nih.gov (S.R.), elke.buschbeck@uc.edu (E.K.B.) https://doi.org/10.1016/j.cub.2024.02.052

SUMMARY

For eyes to maintain optimal focus, precise coordination is required between lens optics and retina position, a mechanism that in vertebrates is governed by genetics, visual feedback, and possibly intraocular pressure (IOP). While the underlying processes have been intensely studied in vertebrates, they remain elusive in arthropods, though visual feedback may be unimportant. How do arthropod eyes remain functional while undergoing substantial growth? Here, we test whether a common physiological process, osmoregulation, could regulate growth in the sophisticated camera-type eyes of the predatory larvae of *Thermonectus marmoratus* diving beetles. Upon molting, their eye tubes elongate in less than an hour, and osmotic pressure measurements reveal that this growth is preceded by a transient increase in hemolymph osmotic pressure. Histological evaluation of support cells that determine the lens-to-retina spacing reveals swelling rather than the addition of new cells. In addition, as expected, treating larvae with hyperosmotic media post-molt leads to far-sighted (hyperopic) eyes due to a failure of proper lengthening of the eye tube and results in impaired hunting success. This study suggests that osmoregulation could be of ubiquitous importance for properly focused eyes.

RESULTS

How proper eye growth, with coordination of all involved components, is achieved continues to be an important subject of investigation. Failure of this process leads to images focused in front of the retina (myopia or nearsightedness) or behind the retina (hyperopia or farsightedness)⁴ and causes blindness in \sim 6.8 million people.⁵ A recent and ongoing myopia epidemic⁶ is predicted to render nearly 50% of the world's population myopic by 2050.⁷ Although still debated, a possible driver of postembryonic eye growth in vertebrates is intraocular pressure (IOP).8 Osmotic processes have been implicated in the translation of visually mediated growth into changes in eye axial length. 9,10 In contrast, little to nothing is known about whether IOP can contribute to postembryonic eye growth in invertebrates, even though their somewhat simpler organization allows them to be a tractable and informative experimental model. Changes in hemolymph hydrostatic pressure are already known to be vital for post-molt body size increases in some arthropods, 11,12 including aquatic arthropods¹³ and could, therefore, also influence eye growth. A compelling system for addressing this question is the aquatic larvae of sunburst diving beetles, Thermonectus marmoratus, which undergo dramatic stepwise growth through three instar stages before pupating into adult beetles. They possess highresolution camera-type principal eyes^{14,15} that support a predatory lifestyle. These eyes are primarily composed of corneagenous support cells (SCs) and a highly asymmetric neural retina

that consists of distal and proximal regions (Figure 1A). The transparent portion of the SC cell bodies secrete the lens and form the core of the eye tube, which is functionally equivalent to the vitreous of vertebrate eyes. A pigmented portion of these cells also forms the eye tube border (Figures 1B, 1C, and S1A). From there in at least some cells thin processes appear to extend proximally and to wrap around the retina (as is the case in the Semper cells of *D. melanogaster*¹⁶). During the transition from second to third instar, these principal eyes grow rapidly in two phases. First, within \sim 1 h of molting, the SC-rich eye tube lengthens dramatically (by \sim 30%) along the optical axis, moving the retina away from the original focal point of the lens. Second, the lens itself undergoes a slower reformation phase to re-establish proper focus (emmetropia) in the now-larger eye. 17 The rapidity of eye tube elongation leads us to hypothesize that the SCs expand in size through hypertrophy-for example, by absorbing fluids (Figure S1B), as is known to occur transiently (in a 24 h rhythm) in the vertebrate choroid.1

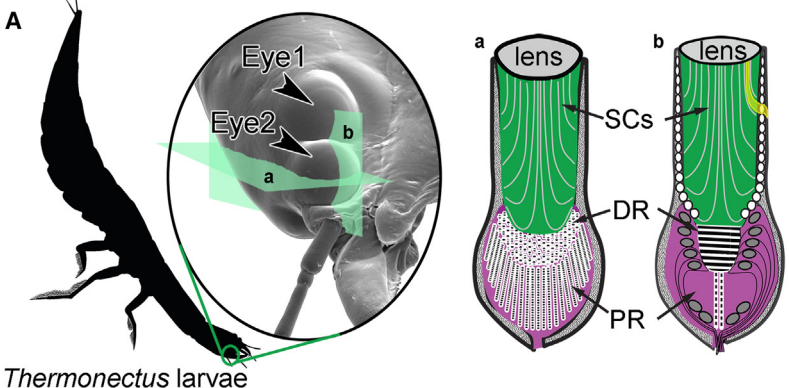
Stable cell counts and transient osmotic pressure changes suggest that osmosis plays a role in eye growth

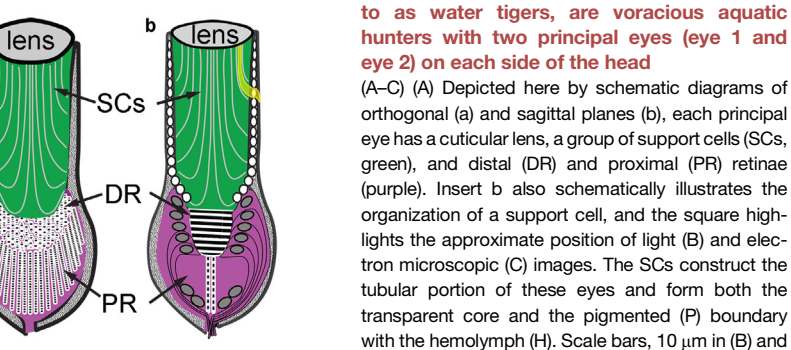
If eye growth in *T. marmoratus* larvae is mediated by osmotically driven swelling of existing cells, then the number of SCs is expected to remain constant. To test for this, we counted and compared DAPI-stained SC nuclei in the two principal eyes of second (Figure 2A) and third (Figure 2B) instars using depth-coded cross sections (Figure 2C). Consistent with our expectation,

CellPress

Current Biology Report

Figure 1. T. marmoratus larvae, often referred





SC SC H

conditions, these larvae live in pond water, which is hypoosmotic compared with the cytoplasm presumably causing SCs to swell upon intake. In contrast, exposure to fluids with higher osmotic pressures is expected to reduce the influx of water into the SCs of the eye tube. This is expected to extend elevated pre-molt osmotic pressures into the post-molt time period, thus inhibiting axial elongation and

5 μm in (C). See also Figure S1.

despite a clear increase in eye size, we found no significant differences between the average SC nucleus counts of second and third instar eyes (Figure 2D).

Cell swelling could be mediated by a transient change in osmotic pressure close to molting. The idea here is that the osmotic pressure in the hemolymph and SCs rises prior to molting, so that after swallowing water, the extracellular fluid becomes an environment of lower osmolarity, which ultimately leads to the influx of water into the SCs and swelling of the eve. To investigate this possibility, we compared the hemolymph osmolality (mOsm/ kg) of larvae at different life stages, ranging from one-day-old second instars to two-day-old third instars (Figure 2E). Consistent with other aquatic insects, 18 the typical hemolymph osmolality of T. marmoratus larvae averaged from about 200 to 360 mOsm/kg at different life stages. Accordingly, a typical insect Ringer's solution 19 with an average osmolality of 428 mOsm/kg was hyperosmotic to the larval hemolymph, but a 50% Ringer's solution was isosmotic with 206 mOsm/kg as the average osmolality (Figure 2E). As predicted, the hemolymph osmolality of larvae that were about to molt was significantly higher than that of larvae that were either a day younger, freshly molted (FM, within 30 min of molting) or a day older (Figure 2E). Taken together, our results on eye-specific SC counts and lifestage-specific osmolarities are consistent with the use of transient changes in osmotic pressure to drive cell size increases in larval eyes through rapid fluid intake.

leading to hyperopia (see Figure S1B). To test our predictions, we exposed larvae to either hyperosmotic (100% insect Ringer's) or isosmotic (50% insect Ringer's) environments for at least 13 h after molting (Figure S2). Measurements of the hemolymph of hyperosmotically treated and control larvae verified that high osmotic pressure was maintained in the treatment group (Figure 2F). Next we assessed their optics with a microophthalmoscope.²⁰ This technique exploits the fact that each of the two principle camera eyes (E1 and E2) on either side of the head (Figure 3A) have a linear, autofluorescent proximal retina that can be live-imaged (Figure 3B) and that the imaging parameters allow assessment of the refractive state of each eye (Figures 3C and 3D). Notably, at the concentrations we used, changes in salinity are known to have negligible effects on the fluid's refractive index21 and hence would not alter the optics in any significant way. In some individuals, certain eyes (0%-12% of controls and 9%-34% of treated larvae; Figures S3A and S3B) were blurry in the ophthalmoscope, regardless of its settings, and therefore excluded from refractive state assessments. The hyperosmotic treatment affected E1 more than E2. As expected, the hyperosmotic treatment led to significantly more hyperopic eyes than observed in the controls (Figure 3C). In contrast, the refractive states of larvae treated with an isosmotic solution were comparable to those of the controls, with a weak (nonsignificant) but consistent hyperopic shift in focus (Figure 3D). To assess the possible effects of these treatments on the optics of the lenses, we also evaluated image formation (Figure S3C). We found no significant difference in focusing properties between the isolated cuticular lenses of hyperosmotically treated and control larvae (Figure S3D). This experimental approach confirmed that refractive states can be influenced by osmotic processes, likely through failure of the

Exposure to a hyperosmotic environment early post-molt leads to hyperopia

If osmotic processes underlie the rapid growth of *T. marmoratus* principal eyes, it should be possible to induce changes in eye size by influencing the osmotic environment. Under normal

Current Biology Report



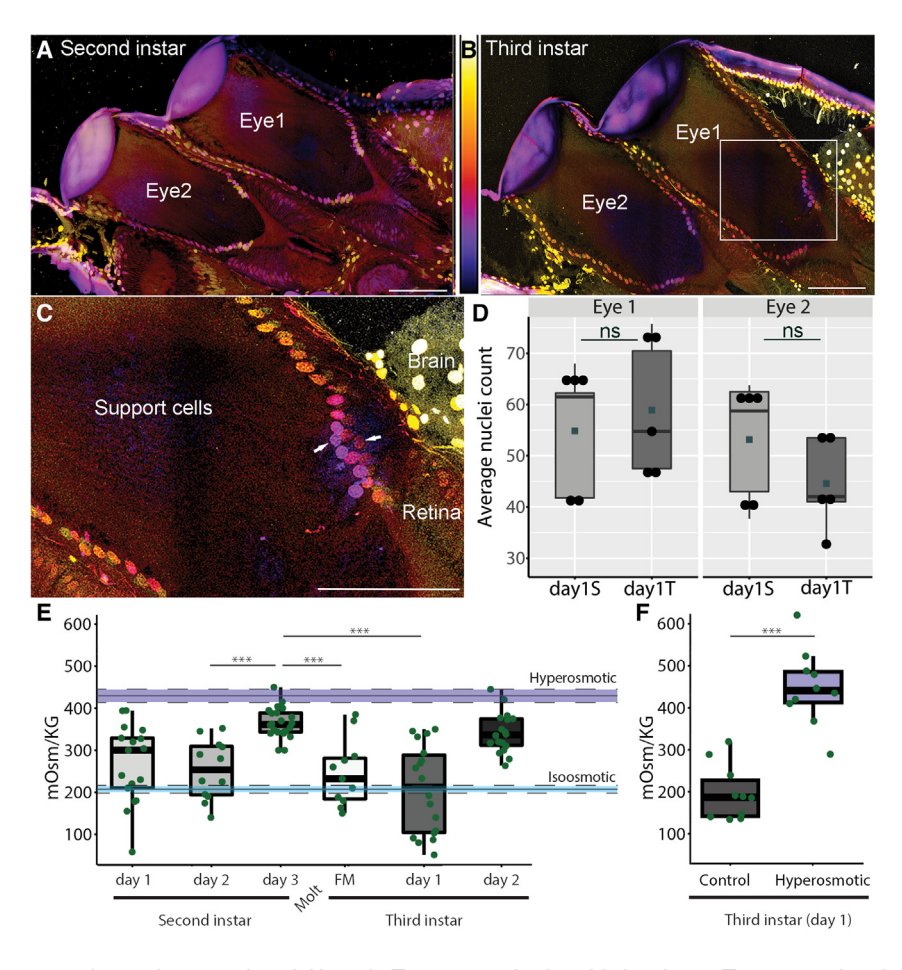


Figure 2. Uniform support cell counts and variable osmotic pressure are consistent with the possibility of osmotically regulated eye growth early post-molt

(A and B) DAPI-stained sections of one-day-old (A) second (day1S) and (B) third (day1T) larvae.

(C) Use of depth coding to accurately identify overlapping nuclei in support cells (arrows).

(D) Cell counts in both eyes are not significantly different between second and third instar individuals (n = 5 for all samples, p_{E1} = 1; p_{E2} = 0.94, unpaired t test).

(E) Measurements of hemolymph osmolality in *T. marmoratus* larvae reveal a significant transient increase in osmolarity preceding molting followed by a significant decrease in osmolality post-molt ($n_{\text{d1S}}=17,\,n_{\text{d2S}}=12,\,n_{\text{d3S}}=22,\,n_{\text{FM}}=11,\,n_{\text{d1T}}=18,\,n_{\text{d2T}}=18;\,p_{\text{d2S-d3S}}=6.3\times10^{-5},\,p_{\text{d3S-FM}}=0.00044,\,p_{\text{d3S-d1T}}=2.2\times10^{-6},\,\text{Wilcoxon's rank-sum test)}.$ Purple and blue lines indicate the osmotic pressure of hyperosmotic and isosmotic solutions that were used for experimental manipulations. FM, freshly molted.

(F) Post-molt treatment with hyperosmotic solution leads to significantly higher post-molt osmotic pressure in the hemolymph. (n = 10, p = 4.3 \times 10 $^{-5}$, Wilcoxon's rank-sum test.) Scale bars, 100 μm . Boxplot whiskers show upper and lower bounds, with the bottom of the boxes representing the bottom 25th percentile, the top representing the 75th percentile, and the middle line representing the median. See also Figure S2.

eye tubes to increase in axial length. To assess whether this level of change is of functional significance, we subsequently tested whether this treatment affected visually guided hunting behavior.

Hyperosmotic treatment causes severe deficits in visually guided hunting behavior

As the hyperosmotic treatment could cause systemic effects, we carefully monitored mortality, postural and/or other anatomical deformities (Figure 4A), and the ability to maintain proper mobility (Figure 4B) and reactivity (Figure 4C). Indeed, compared with 100% of the controls, 83% of the treated larvae survived the hyperosmotic treatment; of these larvae, 6% had deformities and 39% appeared to have postural defects (Figure 4A) and were therefore excluded from further analyses. To ensure that the treatment did not cause significant motor deficits in surviving individuals, we tracked their movement and compared travel distances during the 5 min acclimation period in the horizontal arena. As illustrated in Figures S4A and S4B, the trajectories of control and hyperosmotically treated individuals were comparable, with both preferring to swim along the edges of the arena. In addition, there was no significant difference between the groups in total distance traveled during the acclimation period (Figure 4B), indicating that the hyperosmotic treatment does not simply lead to differences in mobility. Furthermore, the similar numbers of visual responses (Videos S1, S2, and S3; Figure 4C) suggest that the treatment does not simply interfere with the ability to respond to objects.

To assess the visually guided hunting behavior, we obtained video footage of beetle larvae hunting mosquito larvae (prey). While controls consistently struck prey in both arenas (Figures 4D, 4H, S4C, and S4D), the behavior of the hyperosmotically treated larvae was more variable, with a significant reduction in the number of strikes in the vertical arena. Impaired hunting behavior was apparent from the significant reduction in hunting success (Figures 4E and 4I) for the hyperosmotically treated larvae compared with the controls. The hyperosmotically treated larvae also took significantly longer to successfully hunt the first prey item (Figures 4F and 4J). In contrast, the distance from which the strike was initiated did not differ between the two groups (Figures 4G and 4K). Taken together, these data suggest that the hyperosmotic treatment causes significant deficiencies in visually guided hunting behavior.

DISCUSSION

In most animals, postembryonic eye growth is required for the development of an emmetropic eye. The details of this process continue to be an important topic of investigation, ¹ as deficiencies can result in devastating refractive errors ⁴ and blindness. ⁵ Here, we show that osmotic pressure could be an important regulatory mechanism, likely in conjunction with specific molecular pathways, ^{16,22,23} for the establishment of correctly focused invertebrate eyes, with parallels with

CellPress

Current Biology Report

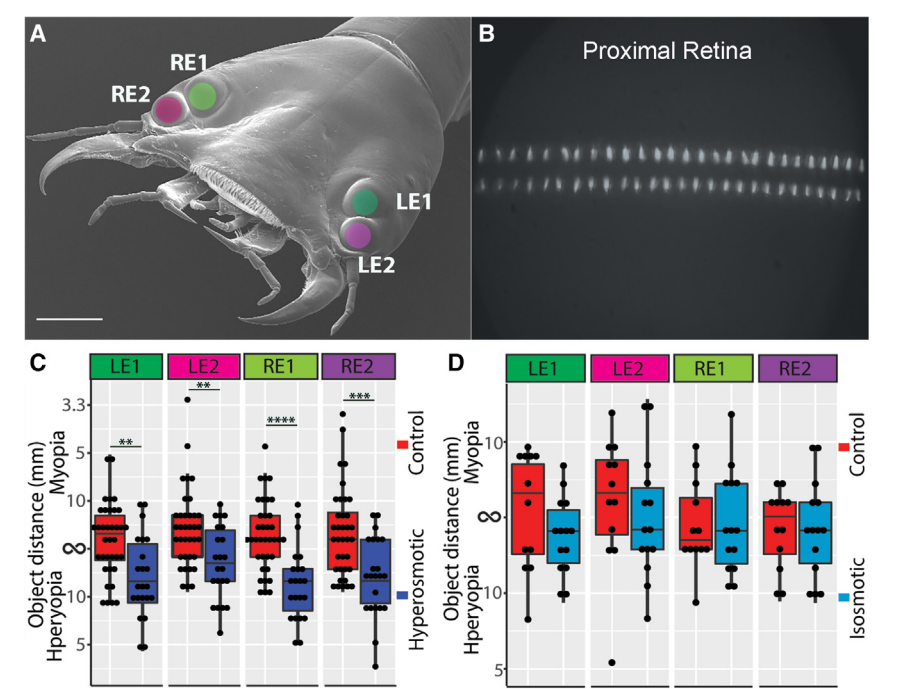


Figure 3. Treating freshly molted larvae with a hyperosmotic solution leads to hyperopia

- (A) T. marmoratus larvae have four principal camera eyes (RE1, RE2, LE1, and LE2, as indicated by colored labels).
- (B) Visualization of the proximal retina with a microophthalmoscope²⁰ was used to assess refractive states
- (C) Treatment with a hyperosmotic solution early post-molt causes a significant hyperopic shift in all eyes compared with control larvae ($n_{Control}=36$, $n_{Hyperosmotic}=22$; $p_{LE1}=0.0044$, $p_{LE2}=0.0044$, $p_{RE1}=6.0\times10^{-4}$, $p_{RE2}=0.0012$, Wilcoxon's rank-sum test).
- (D) In contrast, similar treatment with an isosmotic solution does not result in significant hyperopia ($n_{Control} = 12$, $n_{Isosmotic} = 14$; $p_{LE1} = 0.17$, $p_{LE2} = 0.35$, $p_{RE1} = 0.87$, $p_{RE2} = 0.86$, Wilcoxon's rank-sum test). Scale bars, 500 μ m. Boxplot whiskers show upper and lower bounds, with the bottom of the boxes representing the bottom 25th percentile, the top representing the 75th percentile, and the middle line representing the median. See also Figure S3.

vertebrates, for which the importance of ocular pressure in eye growth regulation has already been recognized.⁸

Our data suggest that the initial rapid increase in the axial length of T. marmoratus camera eyes¹⁷ is caused by SC swelling rather than addition of SCs to the eye tubes (Figures 2A-2D). We propose a mechanism in which the observed pre-molt increase in hemolymph osmotic pressure (Figure 2E) also extends to the eye tubes. Upon swallowing hypoosmotic pond water, the osmotic pressure of the hemolymph is expected to decrease compared with that of the SC cytoplasm, which then favors rapid SC swelling through influx of water. The rapidity of this process, with normal osmotic pressure being reestablished within 30 min of molting (Figure 2E, FM), matches well with osmotically driven cell changes in other systems. 24,25 Interestingly, our data also show a second increase in osmotic pressure at a later stage (day 2), which could be in preparation for the impending transition to the terrestrial environment and metamorphosis. In addition, as expected, the hyperosmotic treatment led to high levels of osmotic pressure in the hemolymph (Figure 2F) and significant hyperopia (Figure 3C). This is likely due to the increased focal length of 3rd instar larval lenses in conjunction with a failure of osmosis-associated SC growth under hyperosmotic conditions, creating a distinct mismatch between lens optics and eye size. Notably, treatment with an isosmotic solution was not sufficient to cause significant refractive errors, raising the possibility that highly efficient osmoregulatory mechanisms are in place to locally balance osmotic conditions (Figure 3C).

Based on our histological investigations, the architecture of SCs in *T. marmoratus* eye tubes form both the core and the border between the eye tubes and the hemolymph (Figure 1B). Therefore, SCs are in a favorable position to be the key mediator of size changes in the eye tube. Cell volume regulation in other systems can also involve cytoskeletal components that impinge mechanical forces on the cell. At the ultrastructural level

(Figures 1C and S1A), no specific cytoskeletal components stand out that would favor such an explanation. Lastly, to determine whether osmotically induced changes in vision could have consequences for fitness, we examined if the hyperosmotic treatment led to significant hunting deficits in the predatory T. marmoratus larvae (Figure 4). While clear deficits were observed in striking behavior (Figures 4D and 4H), hunting success (Figures 4E and 4I), and latency (Figures 4F and 4J), it is notable that no significant differences were observed in the distance from which the beetle larvae attacked their prey (Figures 4G and 4K). This behavior may be related to farsightedness due to underfocused eyes, resulting in no distance at which the larvae could position itself to bring the prey into sharp focus, or to the larvae using binocular distance cues that were unaffected by the treatment. It is important to note that despite our efforts to monitor larval mobility and their ability to detect prey and to exclude any individual that looked or acted abnormally, we cannot eliminate the possibility that the treatment caused additional deficits that influenced hunting success. In fact, the adverse effects of increased salinity on many freshwater invertebrates and the need for a better understanding of related processes have already been noted in the context of freshwater salinization,²⁶ albeit the potential for impaired vision is a novel aspect. Our data raise the possibility that salinization is especially detrimental for freshwater arthropods that rely on visually guided behaviors owing to its impact on the focusing ability of their eyes.

The importance of osmotic processes for the regulation of tissue size and growth

To the best of our knowledge, our work provides the first evidence for osmotic processes being involved in regulating proper focus in an arthropod eye. These findings potentially could relate to circadian changes in eye lengths that are already known in

Current BiologyReport



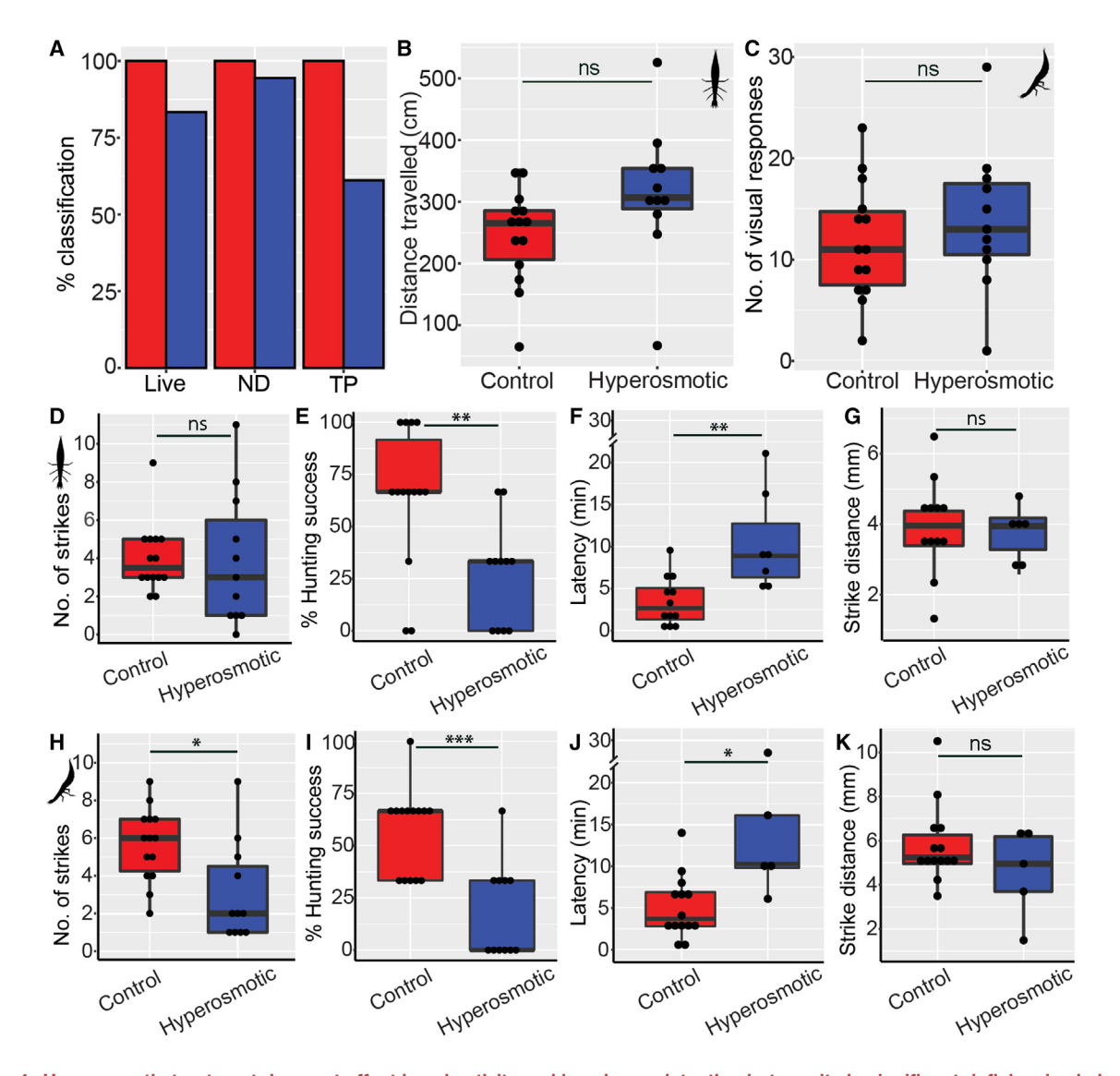


Figure 4. Hyperosmotic treatment does not affect larval activity and larval prey detection but results in significant deficiencies in hunting ability

(A) In contrast to controls, some hyperosmotically treated individuals died or showed anatomical deformities (ND, no deformities) or postural defects (TP, typical posture) and thus were excluded from further analysis.

(B) Treatment with hyperosmotic solution does not influence mobility, as indicated by comparable distances traveled (n_{Control} = 14, n_{Hyperosmotic} = 11; p = 0.1, unpaired t test).

(C) In addition, treatment with hyperosmotic solution does not impair the ability to respond to prey (n_{Control} = 14, n_{Hyperosmotic} = 11; p = 0.43, unpaired t test). Notably, all treated larvae had at least one visual response to a prey item.

(D and H) The number of strikes per individual are comparable between the groups in the horizontal arena ($n_{Control} = 14$, $n_{Hyperosmotic} = 11$; p = 0.51, unpaired t test) but are significantly lower for the treated group in the vertical arena ($n_{Control} = 14$, $n_{Hyperosmotic} = 11$; p = 0.01, unpaired t test).

(E and I) In both arenas, treatment leads to a significant reduction in hunting success (n_{Control} = 14, n_{Hyperosmotic} = 11; p_{Horizontal} = 0.0074, p_{Vertical} = 0.00087, Wilcoxon's rank-sum test).

(F and J) In both arenas, treatment also results in a significantly increased time to capture the first prey item ($n_{Control} = 12$, $n_{Hyperosmotic} = 7$, $p_{Horizontal} = 0.006$; $n_{Control} = 14$, $n_{Hyperosmotic} = 5$, $p_{Vertical} = 0.014$, Wilcoxon's rank-sum test).

(G and K) Despite these deficits, the strike distance is similar for the two groups in both arenas ($n_{Control} = 12$, $n_{Hyperosmotic} = 6$, $p_{Horizontal} = 0.86$; $n_{Control} = 13$, $n_{Hyperosmotic} = 5$, $p_{Vertical} = 0.443$, Wilcoxon's rank-sum test). Boxplot whiskers show upper and lower bounds, with the bottom of the boxes representing the bottom 25th percentile, the top representing the 75th percentile, and the middle line representing the median. See also Figure S4 and Videos S1, S2, andS3.

both vertebrates and insects.^{27,28} Other ways in which osmotic pressure influences ocular parameters are known in vertebrates,¹ such as high IOP resulting in myopia.⁷ Recent studies on frozen chick retinae have revealed a layer-specific differential

ionic gradient, which could establish osmotic gradients *in vivo* and specifically transport water in or out of the tissue, thereby affecting IOP and in turn eye function. Notably, such pressure can be comparable to the force generated by the actomyosin





fibers in cells, as demonstrated in developing zebrafish optic vesicles.³

Could osmotic processes be mediated by eye glia?

Glia are known to be important for water regulation.²⁹⁻³¹ In insect eyes, this cell type is best understood in Drosophila melanogaster, where genetic evidence suggests that Semper cells are resident eye glia, sharing distinct similarities with vertebrate eye-specific Müller glia.²² Müller glia have an osmoregulatory role in maintaining eye function by utilizing water (aqp4) and solute transport (kir4.1) genes.30 Semper cells also express the respective insect orthologs of these aguaporin genes (drip and prip) and ion transport (ncc69 and V-type H+ATPase).²² Whether these genes have a role in water regulation in SCs of T. marmoratus is yet to be tested, but they are known to be important for the osmoregulation of other organ systems in freshwater insects²⁶ and impact immune cell size in insects.³² Thus far, no clear homologies have been established between these cell types of T. marmoratus and those of D. melanogaster. However, based on their evolutionary origin³³ development³⁴ and presence of deeply conserved genetic networks, 23,35-39 homologies or functional equivalence between Semper cells and some SCs may exist. In fact, we recently conducted a tissue-specific transcriptomic analysis of T. marmoratus larval camera eyes and found expression of aquaporins and many ion pumps in SCs. 40 These genes are classically associated with water and ion transport, putting SCs in a good position to regulate fluids within these sophisticated eyes.

Many insect eyes, especially those of predators, ⁴¹ rely on exquisite precision in optical alignment at the microscale, ^{42,43} and how exactly this is achieved developmentally remains an open question. Our data indicate that osmotic pressure could play a key role in this process. As a genetically tractable ⁴⁴ species, *T. marmoratus* provides an important model for relatively easy and noninvasive investigations *in vivo*. Our study highlights the importance of related processes in cell biology and vision, extending their role among both vertebrate and invertebrate systems.

STAR*METHODS

Detailed methods are provided in the online version of this paper and include the following:

- KEY RESOURCES TABLE
- RESOURCE AVAILABILITY
 - Lead contact
 - Materials availability
 - O Data and code availability
- EXPERIMENTAL MODEL DETAILS
- METHOD DETAILS
 - Support cell counts
 - Histological analysis
 - Osmolality measurements
 - Ophthalmoscope imaging and assessment of lens optics
 - Larval behavior
- QUANTIFICATION AND STATISTICAL ANALYSIS

SUPPLEMENTAL INFORMATION

Supplemental information can be found online at https://doi.org/10.1016/j.cub.2024.02.052.

ACKNOWLEDGMENTS

We would like to thank Dr. Annette Stowasser for her initial work and continued advice in this system, Chet Closson at the live microscopy core (LMC, UCMC) for assistance with confocal imaging, Isaac Wolff for assistance with building the larval surveillance setup, Christine Swan and Thiane Thiam for assistance with rearing the beetle larvae, and members of the Buschbeck lab for helpful suggestions. This research was funded by the National Science Foundation under IOS-1856241 (to E.K.B.). Partial support was provided by NIH/NIAID grant R01AI148551 (to J.B.B.).

AUTHOR CONTRIBUTIONS

Conceptualization: S.R. and E.K.B.; data collection: S.R., J.E.L., A.J., and A.T.M.; data curation: S.R., E.K.B., J.E.L., and J.B.B.; data analysis – cell counts and osmolality: S.R., E.K.B., and J.B.B.; lens optics: S.R. and A.T.M.; initial analysis of ophthalmoscope and behavior: S.R.; blind analysis of ophthalmoscope and behavior: R.H.-B. and A.J.; osmolality measurements of hyperosmotically treated larvae: A.T.M. and J.B.B.; manuscript writing and editing: S.R., E.K.B., A.T.M., J.B.B., and J.E.L.

DECLARATION OF INTERESTS

The authors declare no competing interests.

Received: June 30, 2023 Revised: January 30, 2024 Accepted: February 21, 2024 Published: March 20, 2024

REFERENCES

- Troilo, D., Smith, E.L., 3rd, Nickla, D.L., Ashby, R., Tkatchenko, A.V., Ostrin, L.A., Gawne, T.J., Pardue, M.T., Summers, J.A., Kee, C.S., et al. (2019). IMI - Report on Experimental Models of Emmetropization and Myopia. Invest. Ophthalmol. Vis. Sci. 60, M31–M88.
- Owens, M., Giordullo, I., and Buschbeck, E.K. (2020). Establishment of correctly focused eyes may not require visual input in arthropods. J. Exp. Biol. 223, jeb216192.
- Chugh, M., Munjal, A., and Megason, S.G. (2022). Hydrostatic pressure as a driver of cell and tissue morphogenesis. Semin. Cell Dev. Biol. 131, 134–145.
- 4. Harb, E.N., and Wildsoet, C.F. (2019). Origins of Refractive Errors: Environmental and Genetic Factors. Annu. Rev. Vis. Sci. 5, 47–72.
- Naidoo, K.S., Leasher, J., Bourne, R.R., Flaxman, S.R., Jonas, J.B., Keeffe, J., Limburg, H., Pesudovs, K., Price, H., White, R.A., et al. (2016). Global Vision Impairment and Blindness Due to Uncorrected Refractive Error, 1990–2010. Optom. Vis. Sci. 93, 227–234.
- 6. Dolgin, E. (2015). The myopia boom. Nature 519, 276-278.
- Holden, B.A., Fricke, T.R., Wilson, D.A., Jong, M., Naidoo, K.S., Sankaridurg, P., Wong, T.Y., Naduvilath, T.J., and Resnikoff, S. (2016). Global Prevalence of Myopia and High Myopia and Temporal Trends from 2000 through 2050. Ophthalmology 123, 1036–1042.
- Zhang, D., Wang, L., Jin, L., Wen, Y., Zhang, X., Zhang, L., Zhu, H., Wang, Z., Yu, X., Xie, C., et al. (2022). A Review of Intraocular Pressure (IOP) and Axial Myopia. J. Ophthalmol. 2022, 5626479.
- Marshall, A.T., and Crewther, S.G. (2022). Osmotic gradients and transretinal water flow-a quantitative elemental microanalytical study of frozen hydrated chick eyes. Front. Cell. Neurosci. 16, 975313.

Current Biology

Report



- Crewther, S.G., Liang, H., Junghans, B.M., and Crewther, D.P. (2006). Ionic control of ocular growth and refractive change. Proc. Natl. Acad. Sci. USA 103, 15663–15668.
- Cottrell, C.B. (1962). The Imaginal Ecdysis of Blowflies. Observations On the Hydrostatic Mechanisms Involved in Digging and Expansion. J. Exp. Biol. 39, 431–448.
- Nako, J.D., Lee, N.S., and Wright, J.C. (2018). Water vapor absorption allows for volume expansion during molting in *Armadillidiumvulgare* and *Porcelliodilatatus* (Crustacea, Isopoda, Oniscidea). ZooKeys, 459–479.
- deFur, P.L., Nusbaumer, D., and Lewis, R.J. (1988). Physiological Aspects of Molting in Blue Crabs from the Tidal Fresh-Water Potomac River, Virginia. J. Crustac. Biol. 8, 12–19.
- Stowasser, A., and Buschbeck, E.K. (2014). Multitasking in an eye: the unusual organization of the Thermonectus marmoratus principal larval eyes allows for far and near vision and might aid in depth perception. J. Exp. Biol. 217, 2509–2516.
- Stowasser, A., Rapaport, A., Layne, J.E., Morgan, R.C., and Buschbeck, E.K. (2010). Biological bifocal lenses with image separation. Curr. Biol. 20, 1482–1486.
- Charlton-Perkins, M.A., Friedrich, M., and Cook, T.A. (2021). Semper's cells in the insect compound eye: Insights into ocular form and function. Dev. Biol. 479, 126–138.
- Werner, S., and Buschbeck, E.K. (2015). Rapid and step-wise eye growth in molting diving beetle larvae. J. Comp. Physiol. A Neuroethol. Sens. Neural Behav. Physiol. 201, 1091–1102.
- McNamara, J.C., and Freire, C.A. (2022). Strategies of Invertebrate Osmoregulation: An Evolutionary Blueprint for Transmuting into Fresh Water from the Sea. Integr. Comp. Biol. 62, 376–387.
- O'Shea, M., and Adams, M.E. (1981). Pentapeptide (proctolin) associated with an identified neuron. Science 213, 567–569.
- Stowasser, A., Owens, M., and Buschbeck, E.K. (2017). Giving invertebrates an eye exam: an ophthalmoscope that utilizes the autofluorescence of photoreceptors. J. Exp. Biol. 220, 4095–4100.
- Bass, M. (1995). Handbook of Optics: Devices, Measurements, and Properties (McGraw-Hill).
- Charlton-Perkins, M.A., Sendler, E.D., Buschbeck, E.K., and Cook, T.A. (2017). Multifunctional glial support by Semper cells in the Drosophila retina. PLoS Genet. 13. e1006782.
- Rathore, S., Meece, M., Charlton-Perkins, M., Cook, T.A., and Buschbeck, E.K. (2023). Probing the conserved roles of cut in the development and function of optically different insect compound eyes. Front. Cell Dev. Biol. 11, 1104620.
- Cacace, V.I., Finkelsteyn, A.G., Tasso, L.M., Kusnier, C.F., Gomez, K.A., and Fischbarg, J. (2014). Regulatory volume increase and regulatory volume decrease responses in HL-1 atrial myocytes. Cell. Physiol. Biochem. 33, 1745–1757.
- Lindinger, M.I., Leung, M., Trajcevski, K.E., and Hawke, T.J. (2011).
 Volume regulation in mammalian skeletal muscle: the role of sodium-potassium-chloride cotransporters during exposure to hypertonic solutions.
 J. Physiol. 589, 2887–2899.
- Silver, S., and Donini, A. (2021). Physiological responses of freshwater insects to salinity: molecular-, cellular- and organ-level studies. J. Exp. Biol. 224, jeb222190.
- Greiner, B. (2006). Adaptations for nocturnal vision in insect apposition eyes. Int. Rev. Cytol. 250, 1–46.
- Stone, R.A., McGlinn, A.M., Chakraborty, R., Lee, D.C., Yang, V., Elmasri, A., Landis, E., Shaffer, J., Iuvone, P.M., Zheng, X., et al. (2019). Altered ocular parameters from circadian clock gene disruptions. PLoS One 14, e0217111.

- 29. Simard, M., and Nedergaard, M. (2004). The neurobiology of glia in the context of water and ion homeostasis. Neuroscience 129, 877–896.
- Jo, A.O., Ryskamp, D.A., Phuong, T.T.T., Verkman, A.S., Yarishkin, O., MacAulay, N., and Križaj, D. (2015). TRPV4 and AQP4 Channels Synergistically Regulate Cell Volume and Calcium Homeostasis in Retinal Müller Glia. J. Neurosci. 35, 13525–13537.
- 31. Reichenbach, A., and Bringmann, A. (2010). Müller Cells in the Healthy and Diseased Retina (Springer).
- Ahmed, S., and Kim, Y. (2019). An aquaporin mediates cell shape change required for cellular immunity in the beet armyworm, Spodoptera exigua. Sci. Rep. 9, 4988.
- Buschbeck, E.K. (2014). Escaping compound eye ancestry: the evolution of single-chamber eyes in holometabolous larvae. J. Exp. Biol. 217, 2818–2824.
- 34. Stecher, N., Stowasser, A., Stahl, A., and Buschbeck, E.K. (2016). Embryonic development of the larval eyes of the Sunburst Diving Beetle, Thermonectus marmoratus (Insecta: Dytiscidae): a morphological study. Evol. Dev. 18, 216–228.
- Gehring, W.J. (2001). The genetic control of eye development and its implications for the evolution of the various eye-types. Zoology (Jena) 104, 171–183.
- Arendt, D. (2003). Evolution of eyes and photoreceptor cell types. Int. J. Dev. Biol. 47, 563–571.
- Oakley, T.H. (2003). The eye as a replicating and diverging, modular developmental unit. Trends Ecol. Evol. 18, 623–627.
- Kumar, J.P. (2010). Retinal determination the beginning of eye development. Curr. Top. Dev. Biol. 93, 1–28.
- Koenig, K.M., and Gross, J.M. (2020). Evolution and development of complex eyes: a celebration of diversity. Development 147, dev182923.
- Rathore, S., Stahl, A., Benoit, J.B., and Buschbeck, E.K. (2023). Exploring the molecular makeup of support cells in insect camera eyes. BMC Genomics 24, 702.
- Gonzalez-Bellido, P.T., Talley, J., and Buschbeck, E.K. (2022). Evolution of visual system specialization in predatory arthropods. Curr. Opin. Insect Sci. 52, 100914.
- 42. Land, M.F., and Nilsson, D.-E. (2012). Animal Eyes (OUP Oxford).
- Meece, M., Rathore, S., and Buschbeck, E.K. (2021). Stark trade-offs and elegant solutions in arthropod visual systems. J. Exp. Biol. 224, jeb215541.
- 44. Rathore, S., Hassert, J., Clark-Hachtel, C.M., Stahl, A., Tomoyasu, Y., and Bushbeck, E.K. (2020). RNA Interference in Aquatic Beetles as a Powerful Tool for Manipulating Gene Expression at Specific Developmental Time Points. J. Vis. Exp. x, e61477.
- Schindelin, J., Arganda-Carreras, I., Frise, E., Kaynig, V., Longair, M., Pietzsch, T., Preibisch, S., Rueden, C., Saalfeld, S., Schmid, B., et al. (2012). Fiji: an open-source platform for biological-image analysis. Nat. Methods 9, 676–682.
- Buschbeck, E.K., Sbita, S.J., and Morgan, R.C. (2007). Scanning behavior by larvae of the predacious diving beetle, Thermonectus marmoratus (Coleoptera: Dytiscidae) enlarges visual field prior to prey capture. J. Comp. Physiol. A Neuroethol. Sens. Neural Behav. Physiol. 193, 973-982
- 47. R Core Team (2020). R: A Language and Environment for Statistical Computing (R Foundation for Statistical Computing). https://www. R-project.org/.
- 48. RStudio Team (2020). RStudio: Integrated Development for R (RStudio, PBC). http://www.rstudio.com/.





STAR***METHODS**

KEY RESOURCES TABLE

REAGENT or RESOURCE	SOURCE	IDENTIFIER
Reagents		
Sodium chloride	FisherChemical	CAS# 7647145
Calcium chloride dihydrate	FisherBiotech	CAS# 10035048
Sodium bicarbonate	FisherChemical	CAS# 144558
Magnesium chloride	FisherBiotech	CAS# 7791186
Trehalose	FisherBioreagents	CAS# 6138234
TES (N-Tris-(Hydroxylmethyl) Methyl-2-Amino Ethane Sulfonic Acid	FisherBiotech	CAS# 7365448
Sucrose	FisherChemical	CAS# 57501
Paraformaldehyde	Electron Microscopy Sciences	CAT# 15710S
Glutaraldehyde	Electron Microscopy Sciences	CAT# 162210
Tannic acid	Mallinckrodt	CAS# G91 R-1
Sorensen's phosphate buffer	Electron Microscopy Sciences	CAT# 1160005
Ethyl Gallate	Fluka Chemika (Sigma-Aldrich)	EC No. 2126085
Osmium Tetroxide 4% aqueous solution	Electron Microscopy Sciences	CAS# 19150
Uranyl Acetate	Fischer Chemical	CAS# 6159-44-0
Ultra-low viscosity embedding kit	Electron Microscopy Sciences	CAT# 17706-1
DAPI	Roche	REF 10236276001
Instruments		
Ultracut E Microtome	Reichert-Jung	Model 701701
DIC microscope	Olympus	Model BX51
Transmission electron microscope	Hitachi	Model H-7650
Custom-made micro-ophthalmoscope	N/A	Described in Ref. Stowasser et al. ²⁰
Confocal microscope	Zeiss	LSM 710
Osmometer	VAPRO	Model 5600
Sony 4K handycam	Sony US	Model AX53
Incubator	Percival scientific	136LL
Softwares		
R-4.3.1	https://www.r-project.org/	N/A
R studio 4.0.3	https://posit.co/download/rstudio-desktop/	N/A
FIJI 1.54b	https://fiji.sc/	N/A
Z-stack Depth Colorcode 0.0.2	https://github.com/UU-cellbiology/Zstack DepthColorCode	N/A
Yawcam 0.7.0	https://www.yawcam.com/	N/A
MATLAB	MathWorks	license # 41161862
Adobe Photoshop	Adobe	order ADB128270068EDU
Adobe illustrator	Adobe	order ADB128270068EDU
Code		
MATLAB code for activity tracking	Buschebeck lab Github	https://github.com/buschbeck/Osmosis-paper
R code for data analysis	Buschebeck lab Github	https://github.com/buschbeck/Osmosis-paper

RESOURCE AVAILABILITY

Lead contact

Further information and requests for resources and reagents should be directed to and will be fulfilled by the lead contact, Elke K. Buschbeck (elke.buschbeck@uc.edu)

Current Biology Report



Materials availability

This study did not generate new reagents or materials.

Data and code availability

Key data are available in the main text and supplemental infromation. Additional data such as code used for analysis is available on the Buschbeck lab GitHub page (https://github.com/buschbeck/Osmosis-paper, see also key resources table). Further questions should be directed to the lead contact.

EXPERIMENTAL MODEL DETAILS

All larvae were collected and separated from an in-house *T. marmoratus* colony as first instars. Since the larvae are cannibalistic, they were housed in individual enclosures and reared on a diet consisting of gut-loaded blood worms, brine shrimp, and live mosquito larvae (*Aedes aegypti*). Beetle larvae were maintained at 25–28 °C with a 14 h:10 h light:dark cycle. Larvae used for experiments were separated from the colony at the late second instar stage for video observation to monitor molt times.

METHOD DETAILS

Support cell counts

One-day-old second and third instar larval heads were dissected and fixed in 4% paraformaldehyde (EMS) overnight at 4 $^{\circ}$ C. Fixed heads were bisected and embedded in Neg50 and cryosectioned at 15 μ m. Sections were collected on slides and then dried, washed in PBS, and mounted in Fluoromount with DAPI (Thermo Fisher, Cat # 00-4959-52). Tiled Z stacks were obtained using a confocal microscope (Zeiss LSM710 Live Duo microscope) at a pixel size of 0.59 μ m. To enable accurate support cell nuclei counts at different depths, each Z stack was depth-coded using Z-stack Depth Colorcode 0.0.2 in FIJI (Version 1.54b)⁴⁵ to render a 3D image using the default settings. In each sample, individual SC nuclei were counted in four sections, which covered the majority of both principal eyes (E1 and E2) in both larval instar stages. The average SC nuclei counts/section for each biological eye replicate were plotted on R using ggplot2.

Histological analysis

One day old third instar larvae were dissected, fixed and prepared following previously established protocols for general histology¹⁷ as well as transmission electron microscopy (TEM).²³ For general histology, images were acquired with a DIC microscope (Nomarski Optics, Olympus BX51 microscope with a 100x Uplan objective). TEM images were acquired with a transmission electron microscope (Hitachi H-760). Brightness, contrast adjustments and image stitching for TEM images were performed on Adobe photoshop 2023.

Osmolality measurements Larval hemolymph

To assess osmolality levels of larval haemolymph, the following instar stages were used after anesthetizing on ice: one-day-old second, two-day-old second, three-day-old second, freshly molted third, one-day-old third (for both, control animals and animals that were kept in hyperosmotic solution), and two-day-old third. A hole was made in the exoskeleton around the midsection (this area is sufficiently wide to access the hemolymph) and the larva was gently massaged to exude the hemolymph, which was collected in a thin 10 μ l pipette tip and dispensed into a microcentrifuge tube. Immediately after collection, the samples were flash frozen in liquid nitrogen and stored at -80 °C to prevent any changes in hemolymph osmolality. Once all samples were collected, they were thawed and diluted to the required measuring volume of 10 μ l. Osmolality (mOsm/kg) was measured using an osmometer (Vapro Model 5600 vapor pressure osmometer) and the obtained values were corrected for the dilution factor.

Hyper- and isosmotic solutions

To establish a hyperosmotic environment, we used 100% insect Ringer's solution optimized for crickets. ¹⁹ For an isosmotic solution, a 50% dilution of the Ringer's solution was used. The osmolalities of both solutions were determined as described above.

Hyperosmotic treatment of freshly molted larvae

To obtain molted larvae within 30 min postmolt, late-stage second instar individuals were placed under video surveillance in an incubator (Percival Scientific 136LL) at 27 °C, 12 h:12 h dark:light cycle and nocturnal IR illumination. Timestamped images were obtained every minute using freely available surveillance software (Yawcam 0.7.0; https://www.yawcam.com/) and evaluated every 5–10 min (Figures S1A and S1B). Larvae were placed in 100% or 50% Ringer's solution within 30 min of molting (Figure S1C). Control individuals remained in regular pond water until further use.

Ophthalmoscope imaging and assessment of lens optics

The refractive states of *T. marmoratus* larvae were assessed using a custom-made micro-ophthalmoscope. ²⁰ In brief, image series of the retina were captured at different accessory–lens positions, and the best-focused image for each eye was subsequently blindly identified. These positions were used to calculate the optimal object distance for each principal eye. Optical assessments and back focal length measurements of isolated lenses were performed using a modified version of the hanging drop method, as previously described. ¹⁵





Larval behavior

To assess the hunting behavior, hyperosmotically treated and control third instar larvae were left for at least 13 h in the treatment environment and then evaluated through hunting trials. To reduce the three dimensionality of their behavior, larvae were independently evaluated in arenas that restricted vertical (horizontal arena, 7.5 cm × 7.5 cm × 5 cm) or horizontal (vertical arena 10 cm × 1 cm × 8.5 cm) movement, similar to previously described experiments. ⁴⁶ Each trial consisted of 5 min of acclimation followed by 30 min during which larvae were allowed to hunt three *Aedes aegypti* larvae, with 35 min of rest between the two randomly assigned arenas. To assess any motor defects that could be caused by the osmotic treatment, the movements of the larvae were monitored using a MATLAB-based tracking system that established trajectory and travel distance by following the position of the larval heads in the horizontal arena during the acclimation period. To assess the ability of the larvae to detect prey, visual responses to the mosquito larvae were manually recorded in the vertical arena. For each arena, hunting success was calculated as a percentage using the number of prey caught and the number of prey provided. Latency was defined as the time taken to capture the first prey item, and strike distance was established in Fiji (Version 1.54b) as the distance between the mouth parts of the larva and the specific strike site on the prey item. All behavioral assessments were scored blindly.

QUANTIFICATION AND STATISTICAL ANALYSIS

All quantifications and statistical analyses were performed in R⁴⁷ using R.studio version (4.0.3)⁴⁸ (See also key resources table for code availability). Wilcoxon's rank sum test was used for all comparisons except larval mobility and arena specific number of strikes (see Figure 4), in which case an unpaired T-test was used. For all comparisons, a value less than 0.05 was considered to be significant.